Small-angle X-ray scattering investigations of styrene–butadiene–styrene block copolymers during stretching

S. Polizzi*, P. Bösecke, N. Stribeck and H. G. Zachmann†
Institut für Technische und Makromolekulare Chemie, Universität Hamburg, FRG

R. Zietz
MPI für Polymerforschung, Mainz, FRG

and R. Bordeianu
ICECHIM, Bucharest, Romania
(Received 3 October 1988; revised 22 June 1989; accepted 11 September 1989)

A small-angle X-ray scattering study on styrene–butadiene–styrene block copolymers during stretching is reported. Measurements have been performed at the Hamburg Synchrotron Radiation Laboratory at DESY using a two-dimensional position-sensitive detector. A pattern of layer lines perpendicular to the stretching direction with ellipsoidal envelope is obtained. This indicates a good orientation of cylindrical polystyrene domains along the stretching direction. The diameter-to-length ratio of the cylinders was found to be 0.6, the length being approximately 39 nm. The long period of the undrawn sample is about 47 nm. Upon stretching, initially this value increases almost affinely, while for $\lambda > 3$ it tends to reach a constant value. The extension at which the curve bends coincides with the inflection point in the stress–strain curve; at higher values of extension, most of the polybutadiene chains are probably completely stretched and further extension is achieved partly by disruption of the polybutadiene matrix.

(Keywords: small-angle X-ray scattering; synchrotron radiation; styrene–butadiene–styrene; drawing; block copolymers)

INTRODUCTION

The study of the structural changes of thermoplastic elastomers under drawing is of obvious interest from both the scientific and technological points of view.

Small-angle X-ray scattering (SAXS) spectra of extended styrene–butadiene–styrene (SBS) triblock copolymer samples have occasionally been reported in the past[1–3], and recently two rather comprehensive studies on this subject by Pakula *et al.*[4] and Séguéla and Prud'homme[5] have appeared.

The work of Pakula *et al.*[4] reports on samples in which the polystyrene (PS) domains have the form of long rods, which during stretching yield and break. The PS domains assume a preferential orientation inclined to the stretching direction, giving rise to a four-point pattern.

In the paper of Séguéla and Prud'homme[5], samples of hydrogenated SBS (SBS-H) have been investigated, some of them with rod-like PS domains and others with spherical PS domains. For the first kind of sample the results are similar to those of Pakula *et al.*[4], whereas the samples with spherical PS domains give rise to a scattering pattern made up of layer lines perpendicular to the stretching direction. The intensity distribution is spherical.

In the present work, an SBS copolymer with a different fraction of styrene and different molecular weights obtained by spin-casting is investigated, which, as can be seen, shows scattering different from that of the samples studied by other authors. In addition, the kinetics of the orientation is investigated by utilizing a drawing machine designed to work at the polymer beam line at HASYLAB, DESY, Hamburg. The use of synchrotron radiation in connection with a two-dimensional detector has allowed us to carry out fast measurements directly during drawing, so that relaxation is avoided.

Our studies of the samples in the undrawn state are reported in previous publications[6–8]. The results obtained by electron microscopy[8] show that the polystyrene forms cylinders having a diameter $d = 25$ nm and a length $h = 40$ nm. The lateral distance between the centres of gravity of the cylinders is 52 nm. From the poor staining of the polybutadiene (PB) phase surrounding the polystyrene (PS) cylinders, it is concluded that the PB phase is polluted by the polystyrene. SAXS investigations performed by means of a Kratky camera[7] confirm these results. The positions of the scattering peaks are in very good agreement with the lateral distances between the cylinders observed by electron microscopy. The segment length distribution function derived from the angular dependence of the scattering curve has a maximum at about 25 nm, in good agreement with the average diameter of the PS cylinders (25 nm) and the thickness of the intermediate PB phase (27 nm). Finally, the small-angle X-ray scattering power is smaller than that calculated for a two-phase system of pure PB and pure PS, thus proving that phase separation is incomplete.

In addition, SAXS revealed a slight orientation in the undrawn samples, which is negligible, however, in

* Present address: Dipartimento di Chimica-Fisica, Università di Venezia, Italy
† To whom correspondence should be addressed

0032-3861/90/040638-08

comparison with the orientation obtained by elongation reported in this paper. The elongation was performed in the same direction as that of the initial elongation.

EXPERIMENTAL

The polymer investigated is a linear SBS block copolymer. The butadiene blocks have a number-average molecular weight $M_n = 80\,200\,g\,mol^{-1}$, whereas the styrene end-blocks have $M_n = 21\,200\,g\,mol^{-1}$. The synthesis of the material has been described earlier[9]. The polymer film was obtained by spin-casting from toluene solution[9]. The morphology of this undrawn sample was determined in previous investigations[6–8] and is briefly described in the 'Introduction'.

The drawing machine allows the sample to be drawn up to a draw ratio of about $\lambda = 15$ (λ = length of drawn material/initial length). During drawing, the same part of the sample is always maintained in the incident beam. A complete description of the machine has been published elsewhere[10].

The samples had an initial length of 35 mm. They were drawn stepwise ($\lambda = 1, 2, 3, \ldots$) with $0.1\,m\,s^{-1}$ average speed until they slipped out of the sample holder. After each extension step, the scattering pattern was collected during 5 s in a first series, and 60 s in a second one.

The SAXS measurements were performed at the polymer beam line at HASYLAB using the double-focusing camera described earlier[11]. A two-dimensional detector (SIT-Vidicon[12,13]) has been used at a distance of 2.60 m from the sample. In order to monitor the primary beam, besides the usual ionization chamber in the incident beam a second small one had to be built inside the beam stop. This allows the absorption of the sample to be measured *in situ* at different extensions. The thickness during stretching, on the contrary, has been measured separately on an Instron instrument. The value of the absorption coefficient μ obtained is in very good agreement with the one determined for the undrawn sample by the moving-slit method on a Kratky camera.

METHODS OF EVALUATION

The measured scattering intensity was normalized using the following equation:

$$I(\mathbf{s}) = \left(\frac{I'(\mathbf{s})}{I_0\, e^{-\mu t}} - \frac{I_s(\mathbf{s})}{I_{B0}} \right) \frac{S(\mathbf{s})}{t} \qquad (1)$$

Here $I'(\mathbf{s})$ is the measured scattering intensity as a function of the scattering vector $\mathbf{s}$ ($|\mathbf{s}| = 2 \sin \vartheta / \lambda_w$, λ_w being the radiation wavelength and ϑ half the scattering angle); $I(\mathbf{s})$ is the normalized intensity; I_0 is the primary beam intensity as measured by the first ionization chamber; t is the thickness of the sample; and μ is the absorption factor. The transmittance of the sample, $e^{-\mu t}$ is obtained from the ratio of the intensities measured by the two ionization chambers, I'_0/I_0. Also in equation (1), $I_B(\mathbf{s})$ is the background scattering (measured at the end of each drawing experiment) and I_{B0} is the corresponding primary beam intensity; finally $S(\mathbf{s})$ is the position sensitivity function of the detector obtained by measuring the radiation from a ^{55}Fe radiation source.

In the case of stretched samples, the scattered intensity (see *Figure 1*) can be considered to be given by an ellipsoidal particle form factor modulated by layer lines

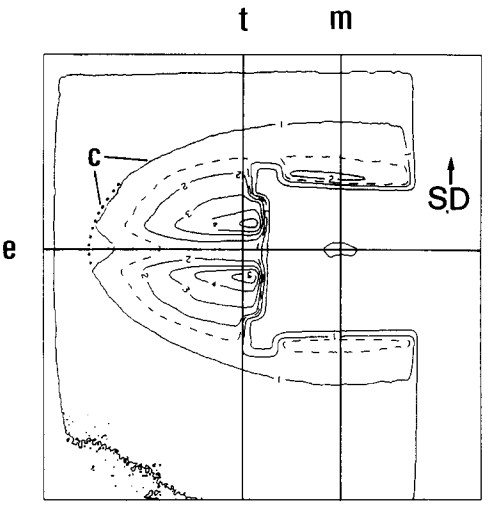

Figure 1 Two-dimensional scattering pattern of an SBS sample stretched to a draw ratio $\lambda = 7$ as obtained by the Vidicon detector. The stretching direction is vertical. The letters c, m and t indicate the curves along which the scattering intensities are considered more closely

arising from interparticle scattering. The ellipsoid representing the intensity distribution has its major axis parallel to the equator and its minor axis parallel to the meridian. This indicates the presence of cylindrical PS domains, which are highly oriented with their axes parallel to the meridian. From the position of the layer lines, we calculated the average separation of the particles. From the intensity distribution, which is governed by the form factor of the particles, we obtained the dimensions of the particles by applying the following considerations.

The two-dimensional particle form factor for non-interfering monodisperse cylinders can be calculated exactly[14]. It follows from the results that the length h and the diameter d of the PS cylinders are given by the two s values s_{0m} and s_{0eq}, where this ellipsoidal envelope vanishes in the meridional and equatorial directions, respectively, by means of the equations:

$$h = 1/s_{0m} \qquad d = 1.17/s_{0eq} \qquad (2)$$

However, the determination of these two points is rather imprecise because of the low signal-to-noise ratio in this scattering region and because of the modulation due to interparticle scattering (the layer lines), especially in the equatorial direction. More precisely, from *any* outer ellipsoidal contour line the diameter-to-length ratio d/h of the cylinder can be obtained[14] by means of the following formula:

$$d/h = 1.17 a_m / a_{eq} \qquad (3)$$

Here, a_{eq} and a_m are half the axes of this outer ellipsoidal contour line along the equator and the meridian, respectively.

Therefore, at different values of extension, initially the ratios d/h were determined by measuring a_{eq} and a_m on iso-level contour plots (c in *Figure 1*) corresponding to a fixed low value of intensity.

In addition, the length h and the diameter d were also determined from this contour plot by replacing, in equation (2), s_{0m} by a_m and s_{0eq} by a_{eq}:

$$h = 1/a_m \qquad d = 1.17/a_{eq} \qquad (4)$$

Of course, this method yields systematically overestimated values of h and d.

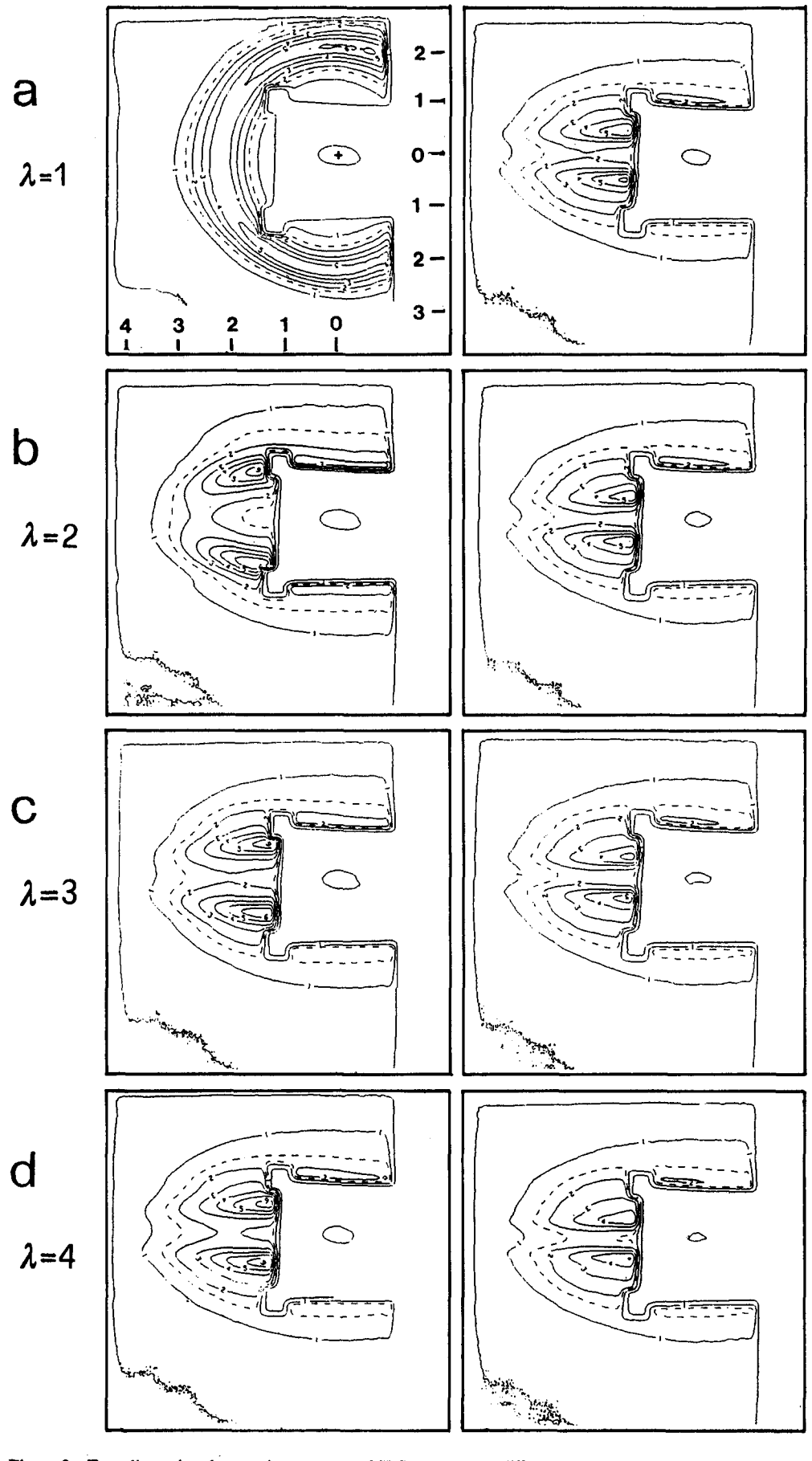

Figure 2 Two-dimensional scattering patterns of SBS stretched to different draw ratios. The patterns were obtained during the first 60 s after quick drawing to λ. The stretching direction is vertical. The two scales in (a) represent the values of $s \times 10^2$ (nm). The same scales apply to (b)–(h)

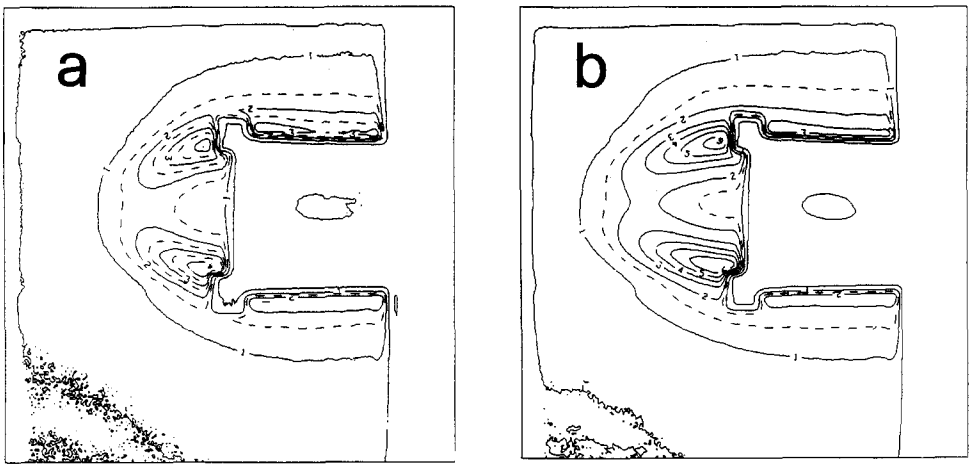

Figure 3 Two-dimensional scattering patterns of SBS stretched to $\lambda = 2$ obtained within the first 5 s after quick drawing (a), compared with that obtained within 60 s (b). The stretching direction is vertical

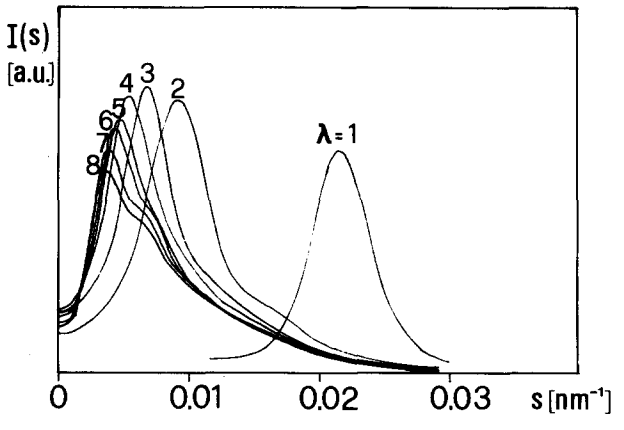

Figure 4 Scattering intensity distribution along a line parallel to the meridian (in *Figure 1*, line m for $\lambda = 1$, line t for $\lambda > 1$) at different extensions. The draw ratio λ is written as a parameter on each curve

Cuts of the two-dimensional patterns parallel to the meridian have been carried out in order to analyse the intensities along this direction. For the undrawn samples, the pattern has been sectioned through the centre of the ring (see line m in *Figure 1*). In the case of the drawn samples, this is not possible because the first layer line is hidden by the beam stop; with these samples, the meridional cut was carried out as close as possible to the beam stop, namely at a distance $s_{eq} = 0.0176\,nm^{-1}$ in the equatorial direction (see line t in *Figure 1*). This method is only possible because the scattering pattern is made up of layer lines. The correctness of this procedure has been tested by comparing the position of the second-order line determined in the cut through the centre with the one in the cut at $s_{eq} = 0.0176\,nm^{-1}$: the difference is less than the experimental error of these measurements.

From the position of the first maximum s_{max}, the average distance between the particles, the long period L_1 in the stretching direction, is calculated by means of the equation:

$$L_1 = 1/s_{max} \qquad (5)$$

We have also fitted the intensities along the cuts by the theoretical particle form factor, which is given along the meridian by $\sin^2(\pi hs)/(\pi hs)^2$ and was used as an approximation along t. From this fit another approximation for the length of the cylinders is obtained, which is compared to the values determined from the contour plot.

RESULTS

Figure 2a shows the scattering of the undrawn sample as detected by the Vidicon. The scattering is concentrated on a ring corresponding to a long period, L, of 47 nm. This is in good agreement with the long period previously determined by using a Kratky camera with a slit focus[6,7]. The scattered intensity along the ring is quite uniform. This clearly indicates that the sample is made up of almost randomly oriented grains, in which the PS domains are regularly arranged. The higher-order rings that one would expect according to the previous measurements[6,7] are outside the detected angular range.

The scattering pattern of the drawn samples measured within 60 s after quick drawing show layer lines with an ellipsoidal intensity distribution (*Figure2b–h*): the layer lines remain perpendicular to the stretching direction (SD). The longitudinal axis of the ellipsoidal intensity distribution is parallel to the layer lines. The presence of layer lines indicates that there exist particles which are regularly arranged in the direction of stretching, while the distances perpendicular to the stretching direction are random. From previous measurements[6,7] it is concluded that the particles are polystyrene domains. The intensity distribution on the layer lines is assumed to be determined by the particle scattering factor alone. Thus, this distribution shows that the particles have an anisotropic shape, i.e. they are cylinders, the length being slightly larger than the diameter. The length of the cylinders is oriented parallel to the stretching direction.

In addition, measurements were also performed within 5 s after stretching. A significant difference between the scattering diagrams measured within 5 s and those measured within 60 s after stretching is observed at $\lambda = 2$ (*Figure 3*). In the fast measurement, the layer lines still have pronounced curvature and the asymmetry of the ellipsoidal envelope is smaller than in the scattering diagram obtained within 60 s. The distance between the layer lines is the same in both diagrams.

In *Figure 4* the intensity distribution along the line t in *Figure 1*, which lies parallel to the meridian, is shown. As expected, the long period increases strongly upon drawing. Furthermore, one can see that, with increasing values of λ, the intensity of the peak first increases (up to $\lambda \approx 3$) and then gradually decreases. The higher-order lines become more evident at larger values of extension. It is interesting to note that the corresponding curves

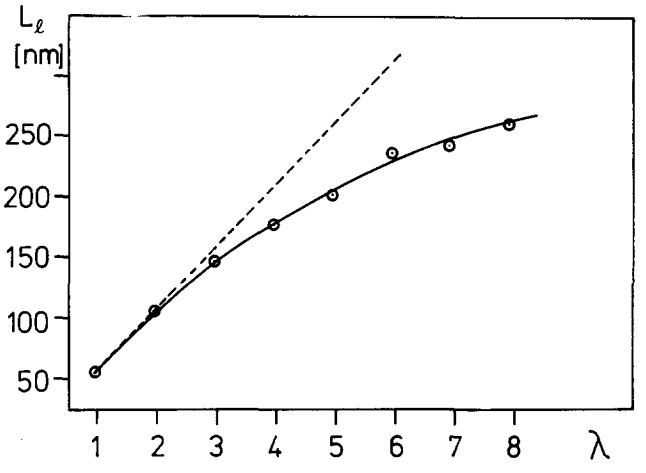

Figure 5 Longitudinal long period L_1 (——) as a function of the draw ratio λ. The line corresponding to affine deformation is also shown (----)

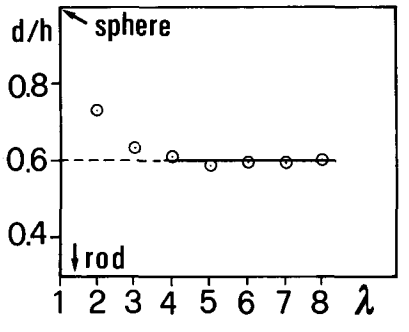

Figure 6 Diameter-to-length ratio d/h of the PS cylinders evaluated from the axes of the ellipsoidal envelope of the patterns in *Figure 2* as a function of the draw ratio λ

obtained within 5 s after stretching do not differ from those in *Figure 4* obtained within 60 s after stretching.

In *Figure 5* the long period in the stretching direction, L_1, given by equation (5), is shown as a function of λ. For the drawn state, this quantity represents the centre-to-centre distance between PS cylindrical domains along their longitudinal dimension. An increase of L_1 on raising λ is observed, which is in agreement with an affine transformation for values of extension up to $\lambda \sim 3$. For larger values of λ, L_1 seems to approach a constant value.

In *Figure 6* the diameter-to-length ratio d/h, obtained by means of equation (3), is plotted as a function of extension. For $\lambda > 3$ this value is constant. For $\lambda = 2$ and 3, the values of d/h seems to be somewhat smaller. This behaviour, however, may be an artefact due to imperfect orientation of the cylinders (see 'Discussion').

Figure 7 shows the values of d and h obtained from the contour plots by means of equation (4). As discussed in the previous section, these values are systematically overestimated. In addition, the values at $\lambda = 2$ and 3 may be affected by imperfect orientation of the cylinders, in the same way as the values of d/h.

Figures 8 and *9* show the scattering intensity distribution along the line t (*Figure 1*) obtained from samples stretched to $\lambda = 2$ and 7, respectively. In addition, curves representing the form factor of a cylinder were fitted to the measured curves at large values of s. The best fit was obtained assuming $h = 32$ nm and $h = 38$ nm, respectively. Owing to the overlap of the particle form factor with the interparticle scattering, such a fit is always delicate. At $\lambda = 7$ the contribution of interparticle scattering shows up at much lower angles, so that a larger part of the form factor is free from interparticle scattering and the fit is more accurate. Moreover, at this extension the cylinders are surely better oriented, so that there is no contribution to the form factor from differently oriented cylinders.

DISCUSSION

Comparison with results of other authors

Our scattering diagrams of the stretched samples show layer lines with maximum intensity on the meridian. From this we have concluded that the PS cylinders are placed with their axes perfectly oriented along lines parallel to the stretching direction SD (*Figure 10a*). The angle α, between the direction of the one-dimensional lattice and SD, and the angle β, between the axis of the cylinders and SD, are both zero. No disruption of the cylinders seems to take place during stretching.

These results are in contrast to those obtained by Pakula *et al.*[4], who found four-point patterns indicating that the angle α, and often β, are different from zero (*Figure 10b*). In addition, disruption of the cylinders seems to take place upon stretching. The scattering patterns of SBS-H samples with cylindrical PS domains presented by Séguéla and Prud'homme[5] are similar to those reported by Pakula *et al.*[4].

We believe that the difference between our results and those in the two publications cited above[4,5] is due to the fact that the diameter-to-length ratio of the domains in the samples investigated in refs. 4 and 5 is much smaller than in our samples. Therefore, with the samples investigated in refs. 4 and 5, orientation is a more complicated mechanism, and disruption of the long PS cylinders is much more probable than with our samples having short PS cylinders. Our samples show an intermediate behaviour between samples with long cylinders and samples containing spherical PS domains also investigated in ref. 5.

Process of deformation

In a consideration of the stretching process, one has to take into account that (i) the PB chains have to be

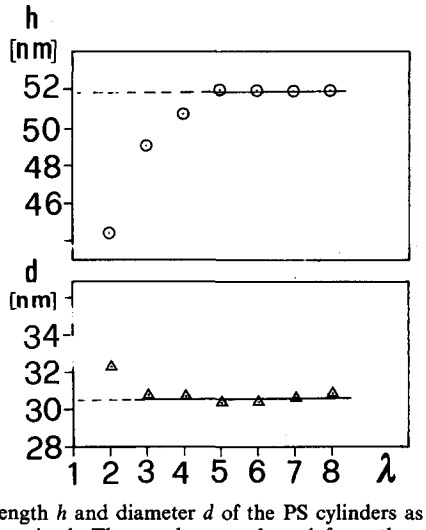

Figure 7 Length h and diameter d of the PS cylinders as a function of the draw ratio λ. These values, evaluated from the axes of the ellipsoidal envelope of the scattering pattern, are considered to be overestimated by approximately 25%

elongated and (ii) the total volume and the densities of the phases must remain almost constant. Therefore, the lateral dimensions have to decrease while the film is elongated in the stretching direction.

In the case of cylinders lying with their long axes perpendicular to the stretching direction, the increase of the distance between two cylinders caused by stretching would lead to a remarkable density decrease in the PB region (see *Figure 11a*), if there is no additional change in the structure. This density decrease can simply be prevented by a rotation of the cylinders by an angle α (see *Figure 11a*). If the thickness of the cylinders is neglected with respect to the distance between the cylinders, the condition for constant volume of the PB region results in:

$$\cos \alpha = 1/\lambda \tag{6}$$

λ being the draw ratio. According to this relation, $\alpha = 75°$ for $\lambda = 4$ and $\alpha = 82°$ for $\lambda = 8$.

If the thickness of the PS cylinders, d, is not negligible compared to the thickness d_B of the PB region between the cylinders, λ has to be replaced by $\lambda(1+r)-r$, where

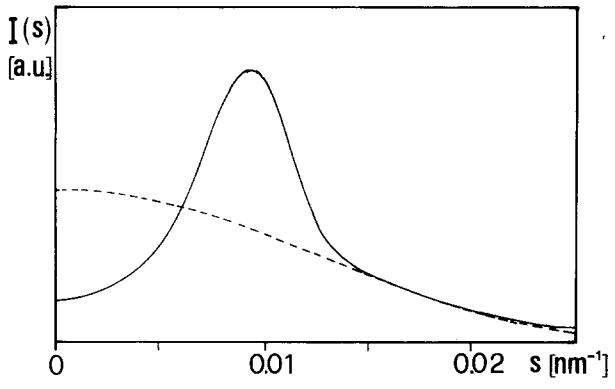

Figure 8 Scattering intensity at $\lambda = 2$ (——) and best fit of the tail of this curve by the form factor of cylinders with $h = 32$ nm (– – – –). In this figure s stands for the component s_m of s in meridional direction at $s_{eq} = 0.0176\,nm^{-1}$

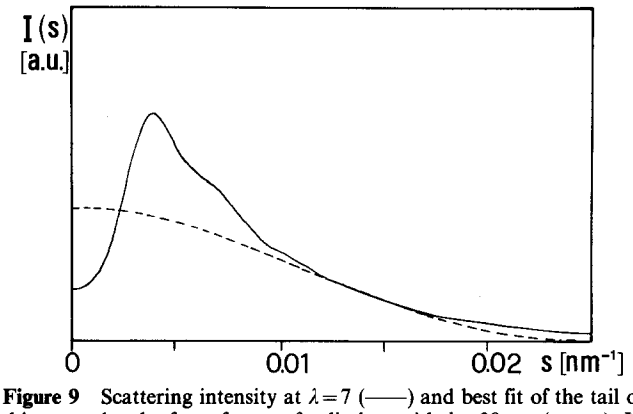

Figure 9 Scattering intensity at $\lambda = 7$ (——) and best fit of the tail of this curve by the form factor of cylinders with $h = 38$ nm (– – – –). In this figure s stands for the component s_m of s in meridional direction at $s_{eq} = 0.0176\,nm^{-1}$

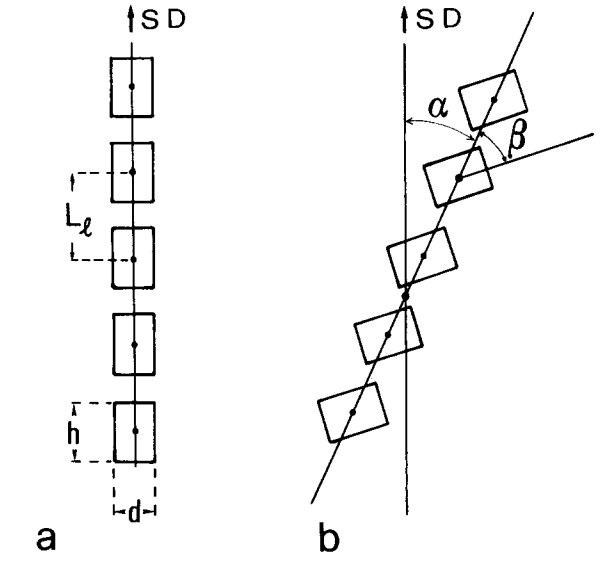

Figure 10 Schematic representation of (a) the arrangement of the cylinders in the extended samples investigated in this work and (b) a possible one-dimensional arrangement of cylinders that are not perfectly oriented[4]

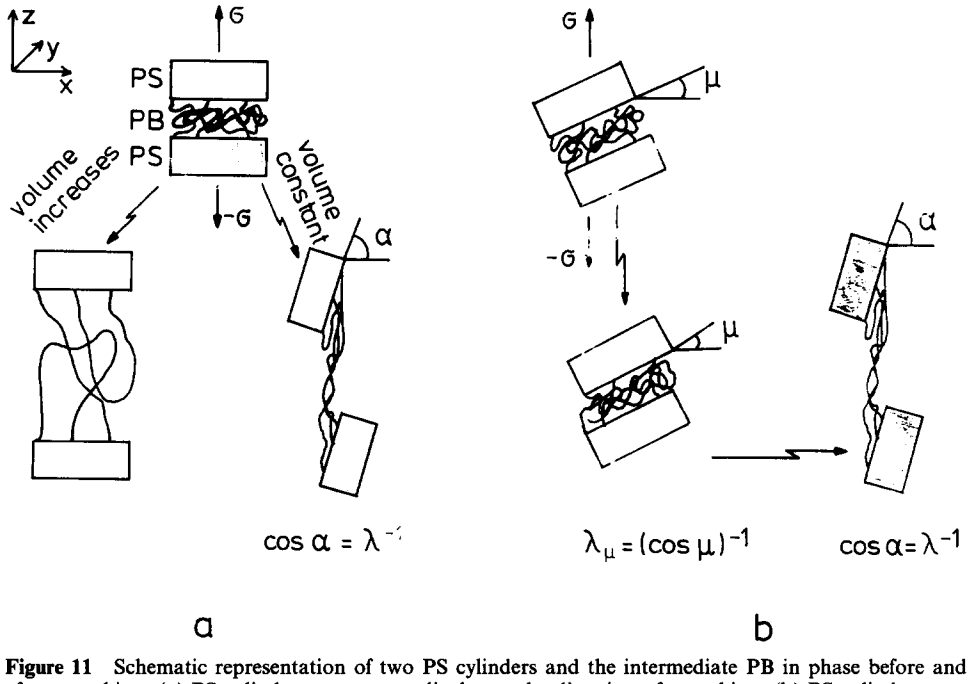

Figure 11 Schematic representation of two PS cylinders and the intermediate PB in phase before and after stretching: (a) PS cylinders stay perpendicular to the direction of stretching; (b) PS cylinders stay at an angle μ to the direction of stretching

$r = d/d_B$. Then the angles α are larger, corresponding to a higher orientation of the cylinder axes in the draw direction.

The rotation of the cylinders considered above results in a decrease of the lateral dimension of the PB domain in the x direction (see *Figure 11a*). In addition, a decrease of the lateral dimension of the PB domain in the y direction may take place. If this is the case, the distances between the cylinders in the y direction decrease and the PB chains connecting these cylinders have to be partly expelled and may enter into the volume of the PB region considered in *Figure 11a*. Then, the angle α does not have to become as large as given by equation (6). If equal size reduction in x and y directions is assumed, equation (6) goes over into:

$$\cos \alpha = (1/\lambda)^{1/2} \tag{7}$$

leading to an angle $\alpha = 69°$ if $\lambda = 8$.

In the case of cylinders not staying perpendicular to the stretching direction, first a shift of the cylinders parallel to their axis will occur. By this shift the chains become elongated by a factor $\lambda_\mu = 1/\cos \mu$, μ being the angle between the cylinder axis and the direction perpendicular to stretching (see *Figure 11b*). This shift is followed by an increase of the distance between the cylinders until the applied stretching ratio λ is reached. The increase of the distance is accompanied by a change of orientation as described in the first case, leading to an orientation angle α that is again given by equation (6), as can be easily shown.

We believe that mainly these mechanisms are responsible for the parallelization of the cylinders in the stretching direction. Owing to these mechanisms, in principle, a four-point diagram is expected, gradually going over into a two-point diagram with increasing λ. The observation of a two-point diagram at comparatively small values of λ may be due to the large broadening of the two scattering points on each layer line, which is caused by the particle form factor.

Any relaxation effects, if they occur at all, would further improve the degree of orientation of the cylinders[15].

Dimensions of the PS cylinders

According to *Figures 6* and *7*, the cylinders seem to shrink in diameter and elongate in length with increasing values of λ up to $\lambda \approx 3$–4. Yet, at least part of this effect could be an artefact caused by incomplete orientation of the cylinders. In fact, if part of the cylinders were not completely oriented in the stretching direction, as a consequence of overlap of differently oriented form factor ellipsoids, this would lead to shorter equatorial and larger meridional axes of the iso-scattering intensity ellipsoid of the scattering pattern. This seems to be confirmed by the noticeable difference observed at $\lambda = 2$ between the 5 s and the 60 s measurements. Apparently, the orientation of the PS domains needs a certain time to take place.

What are the dimensions of the cylinders in the unstretched sample? If the initial trend in *Figures 6* and *7* is only apparent, the extrapolation at $\lambda = 1$ has to be made from the values $\lambda > 4$. In this way, we find that the cylinders in the undrawn samples have a ratio d/h equal to 0.6. Thus, we obtain that the cylinders are rather short.

Concerning the absolute values of h and d, by extrapolation in *Figure 7* we find for the undrawn state $d \approx 31$ nm and $h \approx 52$ nm. Yet, a comparison of the results obtained by the fits in *Figures 8* and *9* indicates that the values in *Figure 7* may be overestimated by approximately 25%. By considering this, one obtains $d \approx 23$ nm and $h \approx 39$ nm. The value of d is in very good agreement with the position of the first maximum in the segment length distribution (25 nm) previously obtained from data collected by means of the Kratky camera[7].

Of course, the results presented in this paper do not exclude the possibility that, in the unextended sample, the cylinders are 'infinitely' long and shorter cylinders are formed by breaking the long cylinders at the beginning of stretching. Our conclusion that the cylinders are short in the unstretched sample, too, relies strongly on the results obtained by electron microscopy[8]. We have performed many cuts in a great variety of directions and we have never observed cylinders longer than 50 nm. The reason for the formation of short cylinders, which, due to surface tension effects, are not favoured by thermodynamics, may be the preparation of samples under technical rather than equilibrium conditions.

Distances between the cylinders

In the highly drawn material, the long period L, determined from the angular position of the SAXS peak (*Figure 5*), to a first approximation represents the distance of the cylinders along their longitudinal axis. In contrast, in the case of the undrawn material, the long period L, determined from the angular position of the SAXS peak, represents, in principle, the average distance of the cylinders in transverse and longitudinal directions, where probably the main contribution arises from the lateral distance L_t. In the following, we try to determine the distance between cylinders along the longitudinal axis for the undrawn sample.

The PS cylinders build up a pseudo-lattice with a rather close structure. In order to perform calculations we have to choose the appropriate lattice. It is known[17] that cylinders tend to build a hexagonal close-packed (h.c.p.) lattice, while spheres build a body-centred cubic (b.c.c.) one. Previous SAXS measurements[6,7] also suggested a weak h.c.p. structure and the addition of paraffinic oil to the sample gives rise to a rather well ordered h.c.p. lattice. For these reasons we used such a lattice (*Figure 12*). As each cell contains one cylinder, the volume fraction ϕ_S of PS is given by the ratio of the volume of one PS cylinder, V_{cyl}, and the volume of the cell, V_{cell}:

$$\phi_S = \frac{V_{cyl}}{V_{cell}} = \frac{\pi(d/2)^2 h}{\sqrt{(3/4)L_t^2 L_l}} \tag{8}$$

From the chemical composition of the material, we know

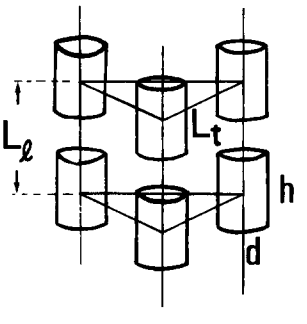

Figure 12 Three-dimensional hexagonal model of the arrangement of the cylinders

that ϕ_S is 0.31. If we take the average long period $L_{av}=47$ nm as an approximation for L_t, we obtain from equation (8) $L_l=55$ nm. This value is very close to the long period L_{av}. This confirms a close-packed arrangement and a small anisotropy of the PS domains.

The assumption that, in the undrawn material, $L_{av} \approx L_t$ is supported by the fact that h is larger than d, and therefore the lateral distance L_t will contribute more strongly to the scattering peak than will the longitudinal distance. In addition, the lateral order may be better than the longitudinal one.

Disruption of the PB phase

If we look at the long period L_l in *Figure 5* using the calculated value for $\lambda=1$, we see that the increase of L_l with λ corresponds to an affine elongation up to $\lambda \approx 3$. At larger elongation, L_l tends to reach a constant value. If we compare this result with the stress–strain curve of this material[6], we notice that the inflection point of the stress–strain curve coincides with the bending point of the curve in *Figure 5*. A similar behaviour is seen in figures 3 and 4 in the publication of Richards and Mullin[16] for styrene–isoprene–styrene samples, but was not discussed by those authors. The deviation of the affine elongation can be explained by a disruption of the PB matrix, probably connected with formation of macroscopic voids.

The change of the scattered intensity with increasing extension also agrees with the assumption of disruption with void formation. As can be seen in *Figure 4*, for $\lambda > 3$ the peak of the normalized scattering intensity starts to decrease with increasing λ, indicating that the scattering volume decreases.

CONCLUSIONS

The unoriented SBS samples investigated show cylindrically shaped PS domains arranged in a close-packed structure with an average distance between the centres of gravity of the cylinders of about 50 nm. The length of the cylinders is approximately 39 nm, the diameter 23 nm. Upon drawing, the deformation is affine up to a draw ratio of about 3. Orientation of the cylinders occurs within less than 60 s and the relaxation effect does not lead to a decrease of the distance between the PS domains. The transition to the non-affine extension region is correlated with the inflection point in the stress–strain curve and is interpreted as a consequence of macrostructural disruption of the PB matrix with void formation.

REFERENCES

1 Pedemonte, E. Dondero, G. and de Candia, G. C. *Polymer* 1975, **16**, 531
2 Hendus, H., Illers, K. H. and Ropte, E. *Kolloid-Z. Z. Polym.* 1967, **216**, 110
3 Brown, D. S., Fulcher, K. U. and Wetton, R. E. *Polym. Lett.* 1970, **8**, 659
4 Pakula, T., Saijo, K., Kawai, H. and Hashimoto, T. *Macromolecules* 1985, **18**, 1294
5 Séguéla, R. and Prud'homme, J. *Macromolecules* 1988, **21**, 635; 1981, **14**, 197; 1978, **11**, 1007
6 Polizzi, S., Stribeck, N., Zachmann, H. G. and Bordeianu, R. *Polym. Compos.* 1988, **9**, 434
7 Polizzi, S., Stribeck, N., Zachmann, H. G. and Bordeianu, R. *Colloid Polym. Sci.* 1989, **267**, 281
8 Hong, D., Stribeck, N. and Zachmann, H. G. to be published
9 Ceausescu, E., Bordeianu, R., Cherchez, I., Ghioca, P., Stancu, R. and Buzdugan, E., 'Forschungen im Bereich der Chemie und Technologie der Polymere', (Ed. E. Ceausescu), Birkhäuser, Basel, 1986, p. 73ff
10 Fischer, E. W., Zietz, R. and Ewen, B. HASYLAB Jahresbericht 319, 1984
11 Elsner, G., Riekel, C. and Zachmann, H. G. *Adv. Polym. Sci.* 1985, **67**, 1
12 Prieske, W., Riekel, C., Koch, M. J. H. and Zachmann, H. G. *Nucl. Instrum. Meth.* 1983, **208**, 435
13 Bösecke, P., Ercan, D. and Riekel, C. *J. Physique Coll.* 1986, **47**, (C5), 175
14 Stribeck, N. *Colloid Polym. Sci.* 1989, **267**, 301
15 Pakula, T., Saijo, K. and Hashimoto, T. *Macromolecules* 1985, **18**, 2037
16 Richards, R. W. and Mullin, J. T. *Mater. Res. Soc. Symp. Proc.* 1987, **79**, 299
17 Alfonso, G. C. and Pedemonte, E. *Polym. Prepr.* 1977, **18**, 276